

## CHARACTERIZATION OF $\text{ZnAl}_2\text{O}_4$ NANOCRYSTALS PREPARED BY COPRECIPITATION AND MICROEMULSION TECHNIQUES

V. Ciupina\*, I. Carazeanu<sup>a</sup>, G. Prodan

Ovidius University, Electron Microscopy Laboratory, 124 Mamaia Blvd., Constantza, Romania

<sup>a</sup>Ovidius University, Chemistry Department, 124 Mamaia Blvd., Constantza, Romania

Nanometer-sized zinc aluminate ( $\text{ZnAl}_2\text{O}_4$ ) particles were synthesized by coprecipitation method using  $\text{NH}_3$  like precipitation agent and the reverse micelle method using like cationic surfactant cetyltrimethylammonium bromide (CTAB), from  $\text{Zn}(\text{NO}_3)_2$  and  $\text{Al}(\text{NO}_3)_3$  an ideal cation stoichiometry for  $\text{ZnAl}_2\text{O}_4$  spinel. XRD analysis for their crystal structure and TEM for their texture characterized the materials obtained after heating at 500 – 800 °C. The TEM photographs reveal that both of them, coprecipitation and the reverse micelle method, are made up of primary nanoparticles in the size range 3-15 nm.

(Received July 21, 2003; accepted November 29, 2004)

*Keywords:* CTAB, Coprecipitation, TEM, HRTEM, XRD, SAED, Scherrer

### 1. Introduction

Nanophase materials composed of discrete grains and the space between the adjacent grains are microstructurally heterogeneous. This heterogeneity, the ratio of the number of atoms present on the surface and inside nanoparticle is triggered by decrease in grain size, leading to many interesting and unusual mechanical, electrical, optical and magnetic properties unknown in the bulk material [1]. This intrinsic properties enhances the importance of nanometer – sized mixed – oxide systems used as ferroelectric, semiconducting and catalytic materials. In the case of semiconductors such as zinc aluminate  $\text{ZnAl}_2\text{O}_4$  the nanoparticles do not possess a conduction band consisting of a plethora of energy levels but have specific and explicit energy levels. Because of this quantization, the bandgap in semiconductor nanoclusters (quantum dots) increases by amount inversely related to the crystallite size. This phenomenon is experimentally manifested as a blue shift in the absorption edge as the particle size decreases.  $\text{ZnAl}_2\text{O}_4$  is well-known wide bandgap semiconductor with a spinel structure [2]. Recent investigation on  $\text{ZnM}_2\text{O}_4$  ( $M = \text{Al}, \text{Ga}$ ) compounds have shown these systems to be new transparent and electroconductive materials [3]. The optical bandgap of polycrystalline  $\text{ZnAl}_2\text{O}_4$  (3.8 eV) indicates that the material is transparent for light possessing wavelengths  $> 320$  nm. Thus,  $\text{ZnAl}_2\text{O}_4$  can be used for ultraviolet (UV) photoelectronic devices [4]. Moreover,  $\text{ZnAl}_2\text{O}_4$  spinel is useful in many catalytic reactions, such as cracking, dehydration, hydrogenation and dehydrogenation reactions [5-10].

The optical and catalytic properties depend crucially on the crystallite size of the material, which has led to a spurt of activity in the preparation of fine  $\text{ZnAl}_2\text{O}_4$  powders.

In this paper we report the synthesis and structural properties of nanometer-sized  $\text{ZnAl}_2\text{O}_4$  synthesized by two routes: coprecipitation method using  $\text{NH}_3$  like precipitation agent and the reverse micelle method using like cationic surfactant cetyltrimethylammonium bromide (CTAB).

---

\* Corresponding author: vciupina@univ-ovidius.ro

## 2. Experimental

### Materials

Chemically homogeneous powders of  $\text{ZnAl}_2\text{O}_4$  have been synthesized from  $\text{Zn}(\text{NO}_3)_2$  and  $\text{Al}(\text{NO}_3)_3$  an ideal cation stoichiometry for  $\text{ZnAl}_2\text{O}_4$  spinel, by two methods: coprecipitation method using  $\text{NH}_3$  like precipitation agent and the reverse micelle method using like cationic surfactant cetyltrimethylammonium bromide (CTAB).

### Methods

The powders were studied by several physical characterization techniques such as X-ray diffraction (XRD) and high-resolution electron microscopy (HRTEM).

In the X-ray diffraction method a Shimadzu XRD 6000 diffractometer with  $\text{CuK}_\alpha$  radiation was used for phase analysis of the fired specimens. High-resolution electron microscopy was used to evaluate the purity and the phase composition of  $\text{ZnAl}_2\text{O}_4$ . The equipment was a Philips CM 120 ST operating at 100 kV and magnification 1200000x. The resolution obtained in our cases was about 2 Å. Lattice plane images gave information about crystal structure and SAED images helped us to identify the phase. The nano - crystals size distribution was investigated.

## 3. Results and discussion

The XRD spectra of the synthesized  $\text{ZnAl}_2\text{O}_4$  powders samples heated at different temperatures, for 2 hours, in dry air are plotted in the Fig. 1. The  $\text{ZnAl}_2\text{O}_4$  was characterized by the main interference peak situated at 2.43 Å, 2.86 Å and 1.42 Å (JCPDS no. 05-0669). Crystallization of the  $\text{ZnAl}_2\text{O}_4$  precursor began at 500 °C. At 800 °C the full crystallization of  $\text{ZnAl}_2\text{O}_4$  was achieved.

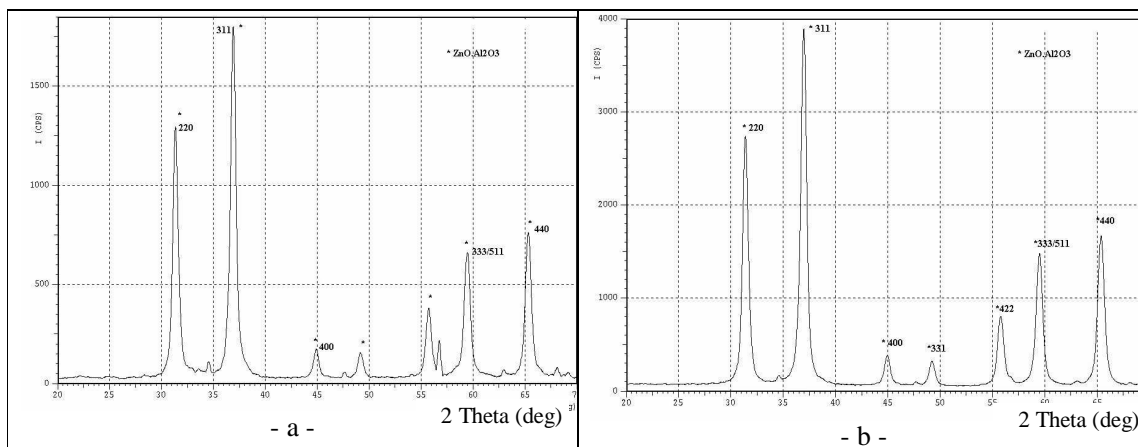


Fig. 1. X-ray diffraction patterns of microcrystalline  $\text{ZnAl}_2\text{O}_4$  powders:  
 a) coprecipitation method – heated at 800 °C, 2 hours;  
 b) reverse micelle method – heated at 700 °C, 2 hours.

Fig. 2 presents the evolution of the main diffraction lines of  $\text{ZnAl}_2\text{O}_4$  heated in the range 500 °C – 800 °C obtained by two methods. One can observe that the formation of  $\text{ZnAl}_2\text{O}_4$  by coprecipitation method is complete at 800 °C and by the reverse micelle method is complete at 700 °C.

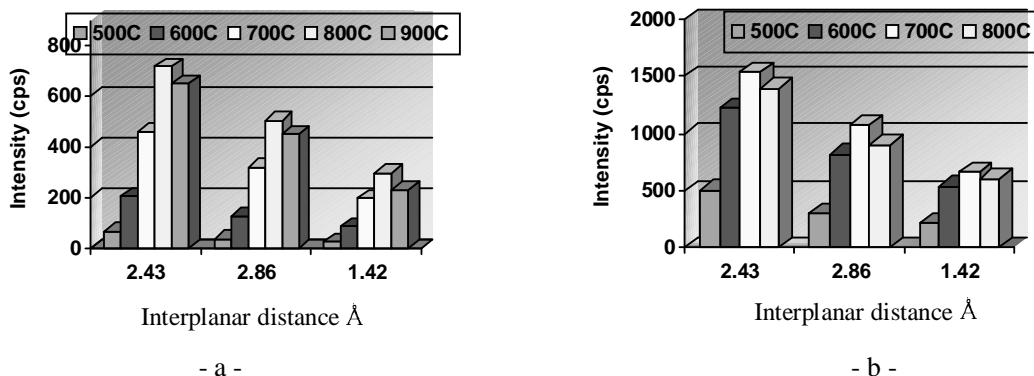


Fig. 2. The evolution of maximum specific interference for ZnAl<sub>2</sub>O<sub>4</sub> powders synthesized by: a) coprecipitation method (NH<sub>3</sub>); b) reverse micelle method (CTAB).

In the Fig. 3 are presented evolution of the intensity of the main diffraction line of ZnAl<sub>2</sub>O<sub>4</sub> synthesized by the two methods.

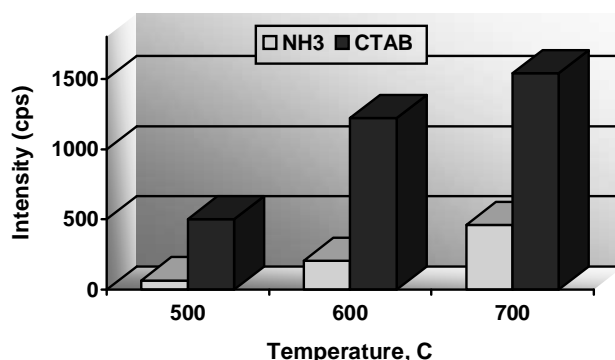


Fig. 3. The intensity evolution of the main diffraction line of ZnAl<sub>2</sub>O<sub>4</sub> (2.43Å) synthesized by the two methods.

The level of crystallization (amount and quality of crystallites) of ZnAl<sub>2</sub>O<sub>4</sub> synthesized by the reverse micelle method is higher than by coprecipitation method.

HRTEM images are used to confirm structure of ZnAl<sub>2</sub>O<sub>4</sub> obtained by XRD. This method is very sensitive to all modification of structure. The measurement of interplanar distance and angle between planes help us to determine the orientation of crystal. These can be made only on images that reveal multiple planes. The following images presents these examinations on ZnAl<sub>2</sub>O<sub>4</sub> obtained at 700 °C for both methods.

Fig. 4 present a single nanocrystalline particle orientated along [011] axis. This results from measurements of interplanar distance and angle between resulted plane identification. The inserts show the FFT space representation for white rectangle area selected on figure. Inserts from particle present a filtered images resulting after applying a blob type filter on FFT representation, separated, left from circle inside and right for circle outside. This methods applied to original image, improves the quality of image, and show features of crystal, e.g. plane (111) and (200) in first case and plane (220), (440) and (331) in second case. The planes (200) appear because double diffraction on crystal. Distortion of images is due to orientation of particle that isn't right along [011], it have a little deviation that induces a deformation of the image.

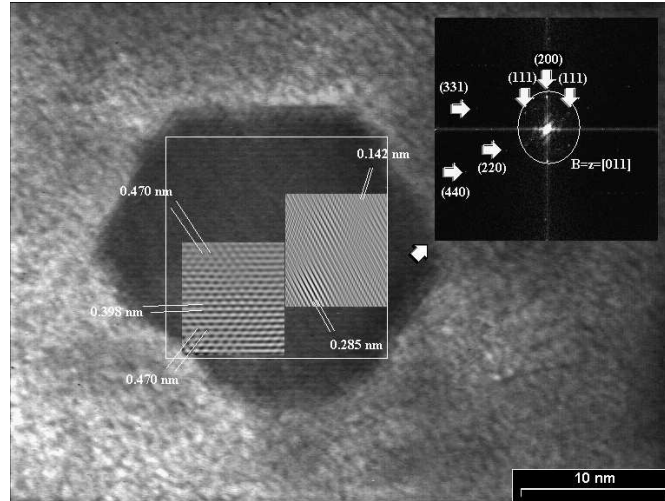


Fig. 4. HRTEM image of single  $\text{ZnAl}_2\text{O}_4$  (coprecipitation method  $700^\circ\text{C}$ ) nanocrystal particle orientated along  $[011]$  axis. The image reveals the presence of  $(111)$ ,  $(200)$ ,  $(331)$ ,  $(220)$  and  $(440)$  planes.

Fig. 5 present a single nanocrystalline particle orientated along  $[-1-43]$  axis. This results from measurements of interplanar distance and angle between different planes. The inserts show the FFT space representation for white rectangle area selected on figure. The right-hand inserts present a filtered image resulting after applying a blob type filter on FFT representation, that masks the initial image and removes the noise. These methods applied to the original image, improve the quality of image, and show hidden features of crystal, e.g. plane  $(335)$  and  $(711)$ . Only, the planes  $(220)$  can be explained by considering a double diffraction on crystal.

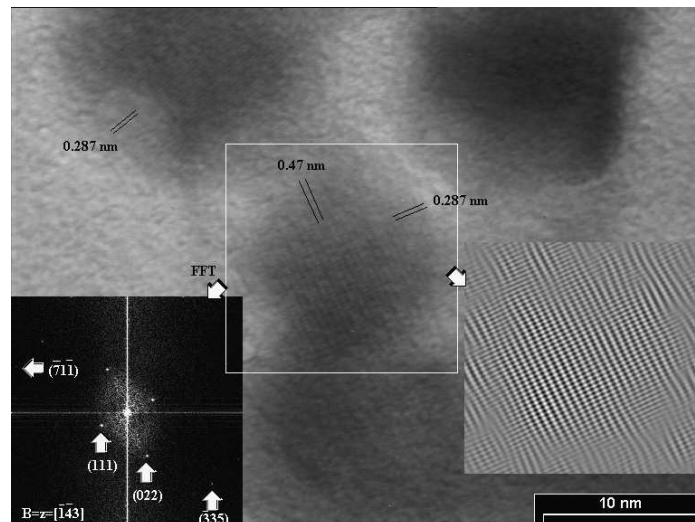


Fig. 5. HRTEM image of single  $\text{ZnAl}_2\text{O}_4$  (reverse micelle method  $700^\circ\text{C}$ ) nanocrystallite obtained from orientated along  $[-1-43]$  axis, that reveal  $(111)$ ,  $(220)$ ,  $(335)$ , and  $(711)$  direction. Inserts present FFT manipulation on image that improve quality of image, and show hidden features of crystal, e.g. plane  $(335)$  and  $(711)$ .

Fig. 6 presents SAED images taken on small area for  $\text{ZnAl}_2\text{O}_4$  (a) coprecipitation method  $700^\circ\text{C}$  and (b) reverse micelle method at  $700^\circ\text{C}$  and reveal the reflections on multiple nanocrystallite.

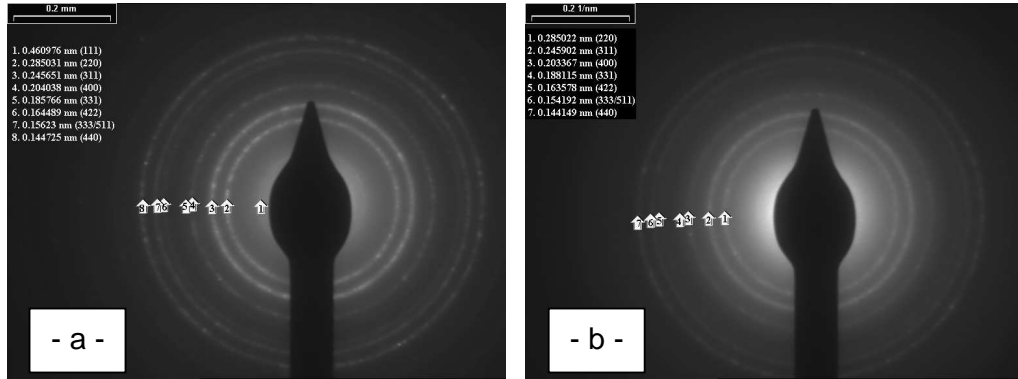


Fig. 6. SAED images for ZnAl<sub>2</sub>O<sub>4</sub> (a) coprecipitation method at 700 °C and (b) reverse micelle method at 700 °C.

The morphology and mean diameter are estimated using BF-TEM micrograph (Fig. 7). The inserts present lognormal distribution curves for mean diameter of the particles. The lognormal function used for fitting the experimental curves is given by:

$$y = Ae^{-\frac{\ln^2(x/x_c)}{2w^2}} \quad (1)$$

where A is an arbitrary constant related to particle number,  $x_c$  represent the distribution maximum and w is strongly correlated with particle diameter dispersion. The results for different temperatures are given in Table 1. Using Scherer relation we can estimate the mean diameter. This relation

$$D = \frac{k \cdot \lambda}{\beta \cdot \cos \theta} \quad (2)$$

implied the use of  $k$  shape factor of particles,  $\beta$  half intensity width and  $\theta$  Bragg angle for the selected ring. We found for (311) ring the size of particles to be about 11 nm, that are confirmed by direct BF image mean diameter estimation. The factor shape was estimated using the same lognormal distribution. The results are compared with those obtained by direct measurement on BF TEM images.

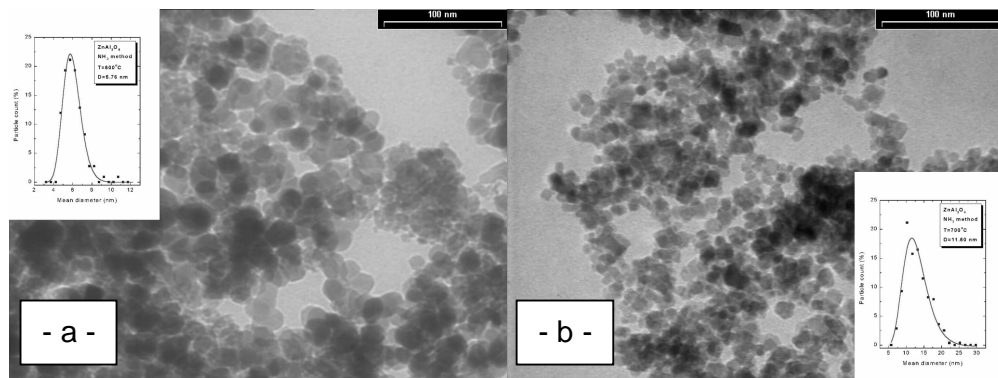


Fig. 7. BF-TEM ZnAl<sub>2</sub>O<sub>4</sub> (a) coprecipitation method at 700 °C and (b) reverse micelle method at 700 °C with lognormal distribution insert .

Table 1. Results of mean size distribution for ZnAl<sub>2</sub>O<sub>4</sub> particles related to specific method of preparation.

Method	Temperature (°C)	y <sub>0</sub>	x <sub>c</sub> (nm)	W	A	D (nm) XRD Scherer
CTAB	500	5.04	10.93	0.23	55.05	6.25
	600	-0.153	3.54	0.23	24.49	10.08
	700	0.75	14.84	0.23	20.25	14.19
NH <sub>3</sub>	500	-0.04	6.65	0.15	25.93	6.97
	600	-0.026	5.75	0.20	22.16	8.29
	700	-0.25	11.60	0.27	18.72	13.96

#### 4. Conclusions

This paper presents an original contribution to the synthesis of ZnAl<sub>2</sub>O<sub>4</sub> powders by the unconventional methods. X-ray diffraction analysis and electronic microscopy were performed for the structural characterization of the synthesized ZnAl<sub>2</sub>O<sub>4</sub>. The results of the analysis lead to the following conclusions:

- ZnAl<sub>2</sub>O<sub>4</sub> can be obtained by thermal treatment at lower temperature at 800 °C.
- The formation of ZnAl<sub>2</sub>O<sub>4</sub> is complete at 700 °C by the reverse micelle method and at 800 °C by coprecipitation method.
- XRD analysis shown high intensity of diffraction peaks of ZnAl<sub>2</sub>O<sub>4</sub> obtained by reverse micelle method that proves the superiority of this method.
- The level of crystallization (amount and quality of crystallites), of ZnAl<sub>2</sub>O<sub>4</sub>, synthesized by the reverse micelle method, is higher than by coprecipitation method.

#### References

- [1] S. Mathur, M. Veith, M. Haas, H. Shen, N. Lecerf, V. Huch, S. Hufner, R. Haberkorn, H. P. Beck, M. Jilavi, *J. Am. Ceram. Soc.* **84**(9), 1921 (2001).
- [2] S. K. Sampath, J. F. Cordaro, *J. Am. Ceram. Soc.* **81**, 649 (1998).
- [3] T. Omata, N. Ueda, H. Kawazoe, *Appl. Phys. Lett.* **64**(9), 1077 (1994).
- [4] T. El-Nabarawy, A. A. Attia, M. N. Alaya, *Mater. Lett.* **24**, 319 (1995).
- [5] J. Wrzyszczyk, M. Zawadzki, J. Trawczynski, H. Grabowska, W. Mista, *J. Appl. Catalysis A: General* **210**, 263 (2001).
- [6] J. Zhao, Z. Wang, L. Wang, Hua Yang, M. Zhao, *J. Mater. Chem. Phys.* **63**, 9 (2000).
- [7] M. A. Valenzuela, P. Bosch, G. Aguilar-Rios, A. Montoya, I. Schifter, *J. Sol-Gel Sci. Technol.* **8**, 107 (1997).
- [8] A. K. Adak, A. Pathak, P. Pramanik, *J. Mater. Sci. Lett.* **17**, 559 (1998).
- [9] Yu-de Wang, Chun-lai Ma, Xiao-dan Sun, Heng-de Li, *J. Inorg. Chem. Com.* **5**, 751 (2002).
- [10] A. E. Giannakas, T. C. Veimakis, A. K. Ladavos, P. N. Trikalitis, P. J. Pomonis, *J. Coll. Interface Sci.* **259**, 244 (2003).
- [11] I. Morjan, R. Alexandrescu, I. Soare, F. Dumitrache, I. Sandu, I. Voicu, A. Crunteanu, E. Vasile, V. Ciupina, S. Martelli, Gas composition in laser pyrolysis of hydrocarbon-based mixtures: influence on soot morphology, *Materials Science and Engineering C* **1020**, 1 (2002).
- [12] X. Batlle, A. Labarta, Finite-size effects in fine particles: magnetic and transport properties, *J. Phys. D: Appl. Phys.* **35**, R15 (2002).